JOURNAL OF MATERIALS SCIENCE 31 (1996) 4493–4501

Diffusion bonding of ferritic oxide dispersion strengthened alloys to austenitic superalloys

M. REES, R. C. HURST
Joint Research Centre, Petten, The Netherlands
J. D. PARKER
Department of Materials Engineering, University of Wales, Swansea, UK

The superior high temperature mechanical strength and oxidation resistance of ferritic oxide dispersion strengthened (ODS) tubular alloys are compromised by the difficulties encountered in joining. Conventional fusion welding techniques generate a weld fusion zone which is devoid of the mechanical strength exhibited by the base material. Therefore, more sophisticated solid state joining techniques, such as diffusion bonding, must be employed when joining ODS materials. This paper describes a series of solid state diffusion bonding experiments carried out between two tubular ferritic ODS alloys and two high temperature austenitic alloys. Careful control of bonding conditions produced pressure retaining joints between one of the tubular ODS alloys and both austenitic alloys. The successful joint design was incorporated into the manufacture of a tubular creep component, which enabled a series of internally pressurized creep tests to be carried out. The microstructure developed at the bond interface of each of the four separate material couples is described and the high temperature performance of the pressure retaining joints is discussed.

1. Introduction

Ferritic oxide dispersion strengthened (ODS) alloys are candidate materials for tubing in an industrial based heat exchanger with an operating temperature range of 1100–1200 °C. These alloys exhibit superior creep strength as a consequence of a fine dispersion of insoluble oxide particles, a large grain size and a large grain aspect ratio (GAR). Excellent creep resistance has been reported in ODS samples when the loading direction is parallel to the major axis of the grains. However, significantly different behaviour would be expected when creep tests are performed with the stress applied perpendicularly to the major axis. Thus, before tubular ferritic ODS alloys can be successfully used in industrial applications, a full characterization of the creep behaviour must be performed.

An additional difficulty which must be overcome before ODS alloys can be used in practice is associated with joining. The mechanical strength and oxidation advantages displayed by ODS alloys under high temperature service conditions can be compromised by metallurgical influences resulting from the joining process. Indeed, conventional joining techniques such as fusion welding are classed as undesirable since even local melting disrupts the elongated grain structure and destroys the dispersion of oxide particles [1]. Moreover, the heat exchanger design under consideration requires the ODS tubing to be joined to an austenitic alloy header. This introduces an additional complexity in that joints with the required performance characteristics must be manufactured between dissimilar materials.

The present work, which formed part of a major European collaborative programme, was involved with performing high temperature creep experiments on selected ODS alloys. The creep strength in different directions was evaluated by conducting experiments under internal pressure with different degrees of axial loading. Moreover, the tubular testpieces were designed with dissimilar joints. Thus, the research undertaken examined potential anisotropy in the tube and creep behaviour of the joint. This paper initially describes a series of critical diffusion bonding experiments between two ferritic tubular ODS alloys, namely MA956 and ODM751, and two dissimilar high temperature austenitic alloys, namely Nimonic 105 and alloy 800H. This work allowed the optimum diffusion bonding parameters to be established, thereby allowing a successful joint design to be incorporated into a full-scale tubular test component suitable for creep testing. The investigation further examines the individual microstructures developed during the bonding process, the implications for overall component design and the high temperature performance of selected joints.

2. Materials characterization

The chemical compositions of the four alloys used in the experimental programme are given in Table I. The

0022–2461

TABLE I Chemical composition of diffusion bonding materials (wt %)

	Fe	Cr	Al	Ti	Y_2O_3	Ni	Co	Mo	Mn	Si
MA956	Bal	20	4.5	0.5	0.5	–	–	–	–	–
ODM 751	Bal	16.5	4.5	0.6	0.5	–	–	1.5	–	–
Nim. 105	1.0	15.7	4.9	1.5	–	Bal	22.0	5.5	1.0	1.0
800H	39.0	23.0	0.6	0.6	–	35.0	–	–	1.5	1.0

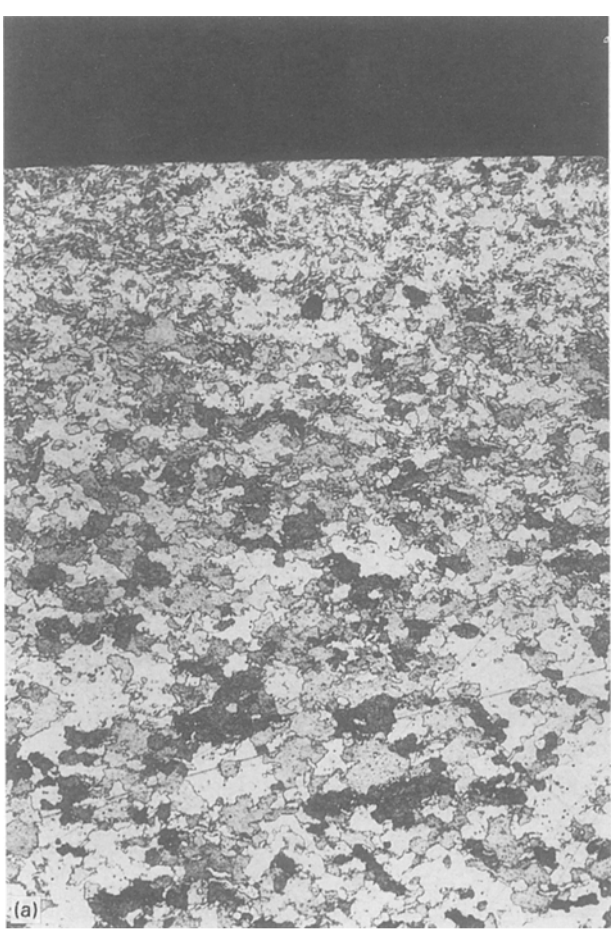

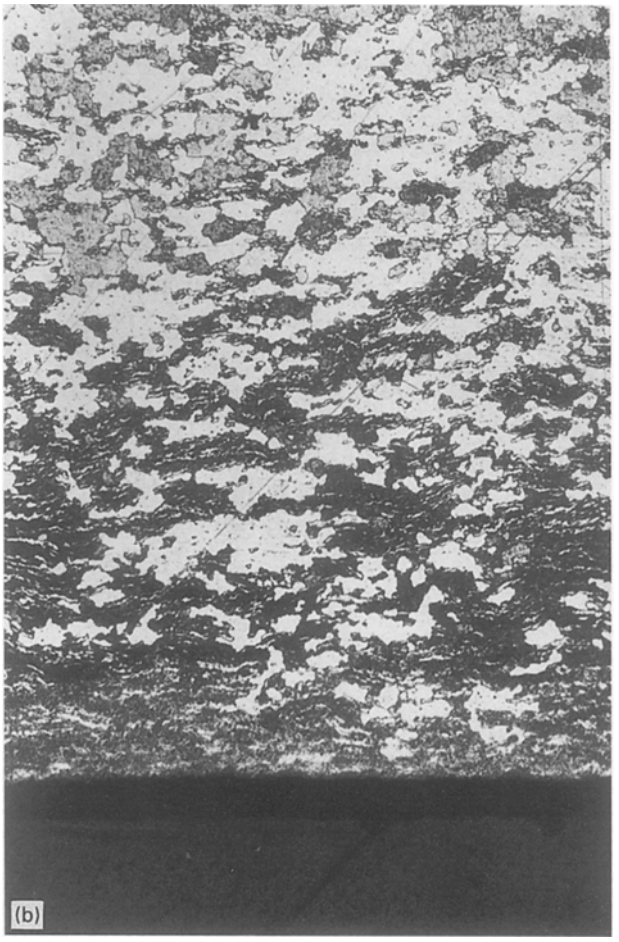

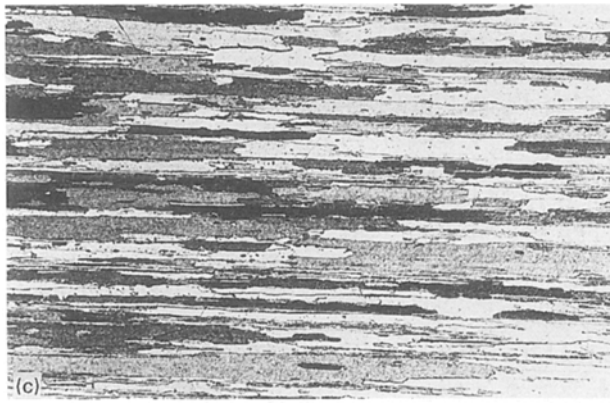

Figure 1 (a) Transverse grain structure at outer surface of MA956 (×100). (b) Transverse grain structure at inner surface of MA956 (×100). (c) Longitudinal grain structure of MA956 (×100).

nominal dimensions of tubular MA956 were 25.4 mm outside diameter with a 1.9 mm wall compared with 27.4 mm outside diameter by 3.1 mm wall for ODM751. Metallographic sections were prepared in both the longitudinal and transverse orientations to determine the grain structure of each tubular alloy.

In the transverse direction, MA956 exhibited irregular shaped grains with serrated interlocking grain boundaries (Fig. 1(a)). In addition, MA956 was classed as being in the partially recrystallized condition as significant quantities of primary recrystallized material were observed throughout the microstructure. The largest concentration of recrystallized grains was situated at the inside surface of the tube (Fig. 1(b)). The average transverse grain size was assessed as being 5–6 ASTM (40–56 μm). In the longitudinal sections the elongated grains exhibited relatively planar boundaries (Fig. 1(c)), with an average longitudinal grain length of 1400 μm. Thus, the average grain aspect ratio (GAR) was approximately 29.

The microstructures of ODM751 in the transverse and longitudinal directions are illustrated in Fig. 2(a) and (b), respectively. As shown, very large grain sizes were present, with transverse grain diameters of

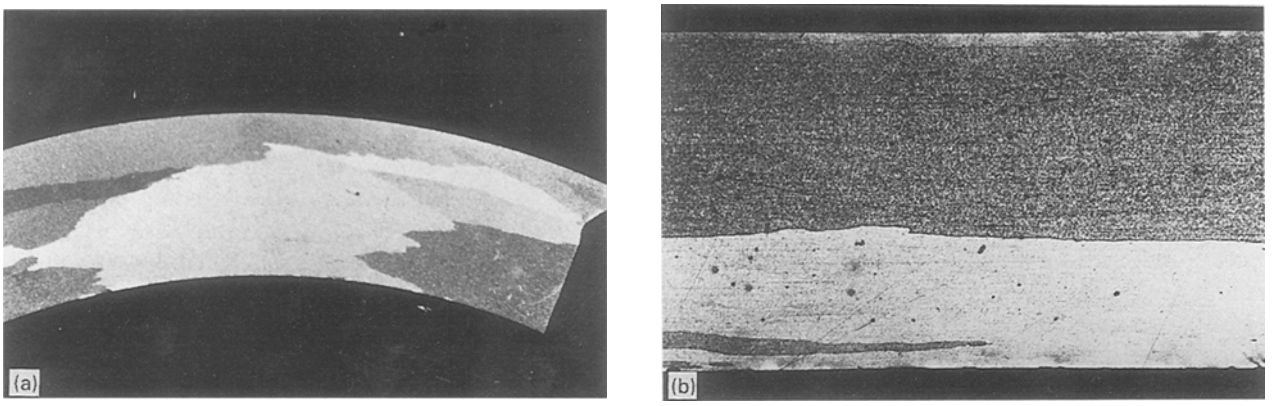

Figure 2 (a) Tranverse grain structure of ODM 751 (×8). (b) Longitudinal grain structure of ODM 751 (×20).

between 0.38–1 mm, and a longitudinal grain length of greater than 60 mm. Thus, for ODM751 the estimated GAR was in excess of 60. The Nimonic 105 and Alloy 800H austenitic alloys displayed equiaxed grain structures, with the average grain diameters assessed as 5–6 ASTM (40–56 μm) and 3–4 ASTM (80–113 μm), respectively.

Transmission electron microscopy (TEM) performed on 3 mm diameter thin films prepared from both MA956 and ODM751 enabled the yttria particle diameter and dispersion to be evaluated. These investigations showed that dimensional similarities existed between the yttria dispersions of the ODS alloys. In both cases, the average particle diameter was in the range between 20–40 nm, with an average particle spacing of between 80 and 110 nm.

3. Experimental procedures

The five factors affecting the quality of diffusion bonds are: the surface quality, the temperature, the interfacial stress, the bonding time and the environment. Based upon available information for MA956 [3], it was decided to undertake diffusion bonding experiments at 1120 °C with exposure for 2 h. The bonding test specimens consisted of a 12 mm long austenitic shaft placed inside a ferritic ODS tube of equal length. The diameter of the shaft was selected to take into account the differing thermal expansion coefficients of the materials involved. The expansion of the austenitic shaft was greater than the ferritic ODS tube (Table II) so that interfacial stresses were created between the two materials at the bonding temperature. A range of diametral clearance/interference conditions were selected to vary the extent of the interfacial stresses developed. Dimensions used ranged from 0.01 mm interference to 0.035 mm clearance. These dimensions were chosen with a view to ensuring that the stresses developed were sufficient to keep the mating surfaces in contact allowing the diffusional processes to occur, but did not cause failure or permanent deformation of the tube.

The contacting surfaces of the test specimens were finely polished by hand, using grade P800 emery paper, whereupon a number of dimensional measurements of the mating surfaces were made and the average diametral value recorded. The individual parts were cleaned in a vibrating ethanol bath to remove any contaminants, whereafter the ODS tube was warmed sufficiently to allow the austenitic shaft to be positioned inside.

TABLE II Material expansion coefficients at 1100 °C

Material	Experimental values		Manufacturers' data
	Hoop	Axial	
MA956	6.6×10^{-6}	5.8×10^{-6}	15.5×10^{-6}
ODM751	6.7×10^{-6}	4.9×10^{-6}	15.0×10^{-6}
Nimonic 105	10.4×10^{-6}	–	19.7×10^{-6}

The diffusion bonding experiments were carried out in a specialized heat treatment rig which enabled test pieces to be heated to temperatures of up to 1200 °C under high vacuum conditions. The test equipment comprised a Carbolite tubular furnace with an alloy 800H work tube connected to a specially fabricated flanged T-junction. The vacuum piping and pressure monitoring systems were secured to this T-junction. The work tube was sealed at the ends with stainless steel covers and a vacuum was created using a rotary and turbo pump system. In all cases, pressures of 10^{-2}–10^{-3} Pa were achieved within 2–3 h. Once the correct pressure range was attained, the specimen temperature was increased at a rate of 20 °C per minute to 1120 °C (± 3 °C), whereupon the temperature was maintained for 2 h. The furnace temperature was controlled by three Eurotherm 810S controllers, while the test piece temperature within the tube was monitored by a single Pt/Pt10Rh thermocouple, positioned through the top end cover and held adjacent to the test specimen. Upon completion of the heat treatment, the furnace was allowed to cool at a controlled rate of 5 °C per minute to room temperature.

Longitudinal and transverse metallographic sections were prepared from each joint. These sections were examined using optical and electron microscopy to document the microstructures present and to assess bond quality. A successful bond was deemed to be a joint where the whole circumferential interface had bonded and fracture of the ODS tube had not

occurred. Once metallography had judged that a successful joint could be produced, it was important to establish if the joint was indeed pressure retaining. This was achieved by manufacturing a tubular specimen using the design illustrated in Fig. 3. The preparation of the test component followed the same procedure as that for the diffusion bonding trials except that the complete assembly was suspended inside the work tube and subjected to the selected diffusion bonding cycle. Upon completion of the heat treatment process, pressure inlet pipes (16 mm diameter by 5 mm wall) were electron beam welded in position and the assembly was leak tested, initially at room temperature, and later at a temperature of 1100 °C. If the tubular specimen proved to be pressure retaining in both instances, longer-term creep exposure was undertaken. Details of the creep data produced in this test programme will be published; however, it should be noted that the joint fabrication procedure developed allowed a series of internally pressurized creep tests on MA956 tubing to be successfully carried out. In each instance, the diffusionally bonded joint remained pressure retaining throughout the duration of the creep test.

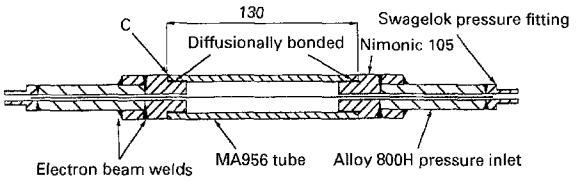

Figure 3 Internally pressurized creep assembly for MA956.

4. Results and discussion

In determining the optimum bonding conditions for joining a ferritic ODS tubular alloy to an austenitic high temperature alloy, a series of diffusion bonding trials were performed where the initial diametral tolerance between the contacting surfaces was systematically varied. The details of the bonding parameters used in joining Nimonic 105 and Alloy 800H to MA956 and ODM751 are given in Tables III and IV, respectively.

Bonding trials were initially carried out on one material couple, namely MA956 to Nimonic 105. The parameters which resulted in successful bonding for these two alloys were used as a starting point in the manufacture of diffusion bonds between the other three alloy pairs.

4.1. Bond formation

Examination of metallographic sections prepared from the MA956/Nimonic 105 test pieces (Experiments 5, 6a and 26) revealed that the whole circumferential joint interface had completely bonded without causing fracture of the MA956 tube. These joints were considered successful. In contrast, Experiments 6b and 6c showed areas of interfacial decohesion and lack of bonding, and were therefore classed as being unsatisfactory. The poor bonding in these tests is related to the relatively large initial diametral clearance used. Thus, the test programme established that successful bonds can be produced between MA956 and Nimonic 105 when the starting diametral tolerance lies in the range of $\pm$ 0.01 mm.

TABLE III Diffusion bonding test parameters for MA956 tube

Specimen code	Shaft material	Bonding temperature (°C)	Diametral tolerance (mm)	Bond classification
5	Nimonic 105	1120	0.005	Successful
6a			0.010	Successful
6b			0.020	Decohesion
6c			0.035	Decohesion
26			− 0.010	Successful
8	800H	1120	0.005	Successful
10			0.010	Successful

TABLE IV Diffusion bonding test parameters for ODM 751 tube

Specimen code	Shaft material	Bonding temperature (°C)	Diametral tolerance (mm)	Bond classification
17	Nimonic 105	1120	0.006	Fracture
19			0.010	Fracture
20			0.010	Fracture
27			0.025	Decohesion and Fracture
29	Nimonic 105	1180	0.020	Fracture
12	800H	1120	0.017	Fracture
22			0.020	Decohesion
23			0.010	Fracture
24			0.015	Fracture

As the thermal expansion coefficients for both Nimonic 105 and Alloy 800H are extremely similar at 1120 °C the joining parameters used to successfully bond MA956 to Nimonic 105 were utilized in bonding MA956 to alloy 800H. Thus, two diffusion bonding tests were carried out between MA956 and alloy 800H (Experiments 8 and 10) with initial diametral tolerances of 0.005 mm and 0.01 mm, respectively. Optical examination of the metallographic sections prepared from both trial tests revealed that successful bonds had been achieved showing that successful diffusion bonds can be produced using a diametral clearance of up to 0.01 mm.

The range of diametral tolerances used in the five bonding trials between the ODM 751 and Nimonic 105 are detailed in Table IV. Although the diametral clearances were the same as those used to produce successful bonds between MA956 and both austenitic alloys, metallographic examination of all the bonding test specimens showed that cracking had developed in the ODM 751 tube. These bonds were therefore classified as unsuccessful. The first bonding trial, Experiment 17, used a diametral clearance of 0.006 mm as a similar tolerance had proved successful in the preceding bonding trials for MA956. Metallographic examination of the joint interface revealed the entire circumference had bonded; however, the joining process had caused the ODM751 tube to fracture (Fig. 4). The intergranular failure of the ODM751 tube suggested that fracture may have resulted from the interfacial stress being too high at the bonding temperature, due to the starting diametral clearance being too small. Hence, further bonding trials were performed where the diametral clearance was progressively increased (Experiments 19, 20 and 27). Post-test metallographic examination of each transverse section revealed that although the joint interface had bonded in Experiments 19 and 20, the bonding process had either fractured the ODM 751 tube in an intergranular manner or produced radial cracking emanating outward from the joint interface (Fig. 5). More notably, when the diametral tolerance was at its largest (Experiment 27) the joint interface separated upon cooling from the bonding temperature and displayed micro-cracking characteristics within the tube similar to those illustrated in Fig. 5.

The diameter of the ODM751 tube was measured prior to and after each diffusion bonding test. However, no measurable post-test diametral strain could be detected in the fractured specimen. Thus, it appears that failure was a consequence of the low ductility of the ODM751 tube at the holding temperature. The bonding temperature was therefore increased to 1180 °C in a bid to increase the ductility of the tubing (Experiment 29). Metallographic examination showed that a good interfacial joint had been achieved, but the tube had fractured in an intergranular manner, similar to Experiments 17 and 19. Again, no measurable increase in diametral strain was detected. Hence, it was concluded that ODM751 could not be diffusionally bonded to Nimonic 105 using the same bonding techniques as employed for MA956.

The details of the diametral clearances used for the four diffusion bonding trials carried out between ODM751 and Alloy 800H are contained in Table IV. Optical examination of the metallographic sections prepared from the test components revealed that all trial tests proved to be unsuccessful. The bonding process either caused fracture of the ODM751 tube or micro-crack development at the inside surface, i.e. the behaviour was similar to the ODM 751/Nimonic 105 failures illustrated in Figs 4 and 5. Moreover, when the diametral clearance was at its largest, the joint interface separated upon cooling from the bonding temperature.

4.2. Microstructural characterization

The metallurgical and structural implications of the successful diffusion bonds were investigated as any potential microstructural weakness could have had a detrimental effect on the performance of a tubular creep component when exposed to internal pressure. The microstructure developed at the MA956/Nimonic 105 joint interface is examined in greatest detail as the microstructure of this bond type proved to be the most complex.

The microstructure developed during the bonding of MA956 to Nimonic 105 is illustrated in Fig. 6. The joint had been used to seal a tubular test component which had been creep tested at 1100 °C for 543 h. The original bond interface is readily identifiable and it is

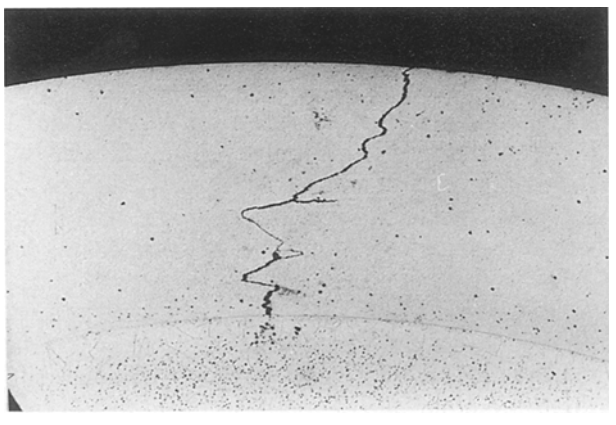

Figure 4 Fracture of diffusionally bonded ODM 751 tube (×20).

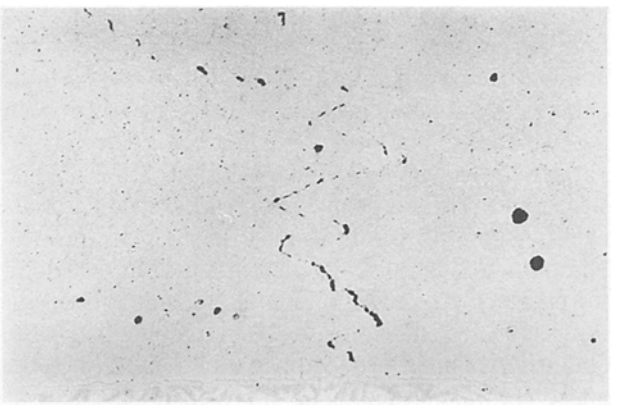

Figure 5 Micro-crack development at joint interface of a diffusionally bonded ODM 751 tube (×160).

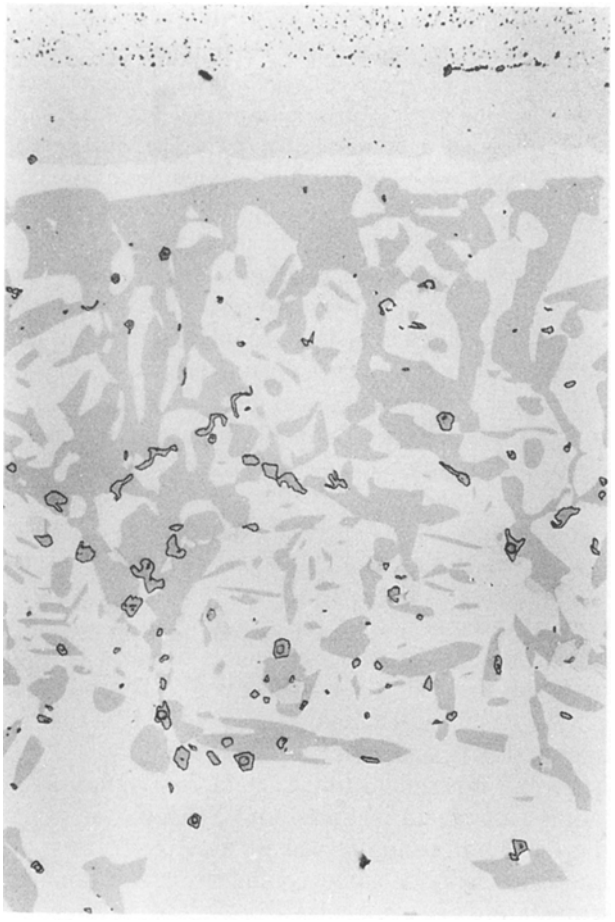

Figure 6 The microstructure present after bonding MA956 to Nimonic 105 (× 200).

clear that intermetallic phases and intermetallic particles have developed on the Nimonic 105 side of the bond interface as a result of the diffusive process. The microstructure developed during the bonding process can be divided into three distinct regions:

(i) the formation of a large intermetallic phase with an inter-dispersion of two phase particles;
(ii) a particle containing intermetallic zone produced at the original bond interface;
(iii) a thin intermetallic band separating the particle containing zone and the intermetallic phase.

A microprobe line scan analysis was carried out on a typical bonded section and the resulting elemental plot is represented in Fig. 7, where the three main metallurgical regions have been identified. The formation of the large intermetallic phase within the Nimonic 105 shaft has been attributed to the sizeable compositional difference in iron that existed between the two alloys. (Nimonic 105 contained 1% iron compared to approximately 70% in MA956; Table I). The steep concentration profile between the two materials results in rapid iron diffusion from MA956 into the Nimonic 105. The iron preferentially diffused along the Nimonic 105 grain boundaries and combined with the other elements to create an intermetallic phase. Quantitative microprobe analysis of the intermetallic phase showed nickel to be the primary element at 44 wt%, whilst the other constituent elements were evaluated at Fe 20%. Al 18%, Cr 5% and Co 8%.

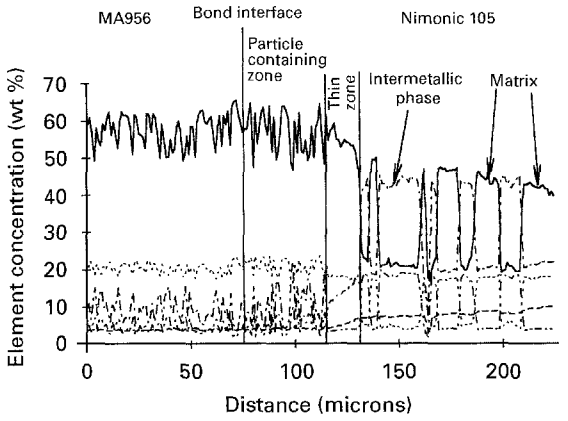

Figure 7 Elemental concentration profiles for Al (— — —), Fe (—), Cr (-------), Ni (— — —) and Co (— — —) across the MA956/Nimonic 105 diffusion bond.

Analysis of the adjacent matrix revealed a contrast in elemental composition, with iron being the largest primary element at 40%, with the other constituent elements measured at Ni 20%, Al 8%, Cr 17% and Co 8%. Hence, it is apparent from this elemental comparison that the intermetallic phase formation required 20% iron and 44% nickel.

The diffusion bonding process also produced a dispersion of two phase particles within the intermetallic phase and the surrounding matrix (Fig. 6). The particles consisted of an inner faceted core surrounded by an outer phase. Compositional analysis of the particles revealed the core to be titanium, and the surrounding phase a combination of molybdenum and titanium. The faceted morphology of the inner titanium core indicated it to be a TiCN particle originally present in the Nimonic 105 structure. The formation of the surrounding phase resulted from the dissolution and diffusion of the MoTi particles originally present in the Nimonic 105 material. This analysis is supported by the observation that a MoTi particle depleted zone existed immediately adjacent to the intermetallic phase within the Nimonic 105 shaft.

A further consequence of the bonding procedure was the development of a particle containing intermetallic zone at the original bond interface. The morphology, chemical composition and structure of the particles were examined by scanning electron microscopy (SEM) and TEM metallographic techniques. The quadrifid and trigonal particle morphologies observed during structural analysis are illustrated in Figs 8 and 9. The presence of gamma prime (γ') particles within the Nimonic 105 structure indicated that the intermetallic particles may have developed by a particle coarsening mechanism similar to the cube on cube corner model described by Westbrook [4] (Fig. 10). However, qualitative chemical analysis showed that the intermetallic particles consisted of aluminium, nickel and iron. The presence of iron indicated that particle formation was related to the diffusive process as iron can partly replace nickel within this structure [5]. Therefore, it is reasonable to assume that the diffusing iron readily combined with the γ' particles already present in the Nimonic 105 forming intermetallic particles in a morphological structure similar to that of the γ' particles. This theory

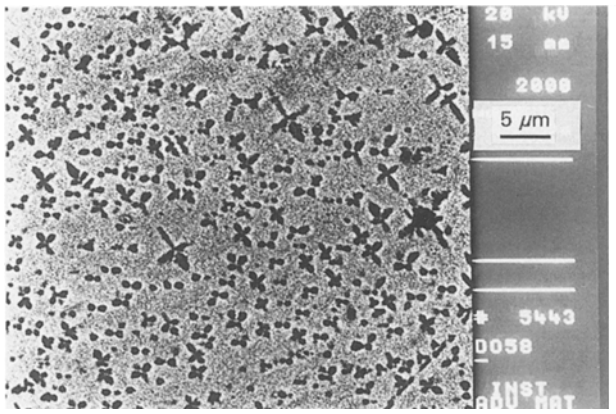

Figure 8 Quadrifid particle morphology.

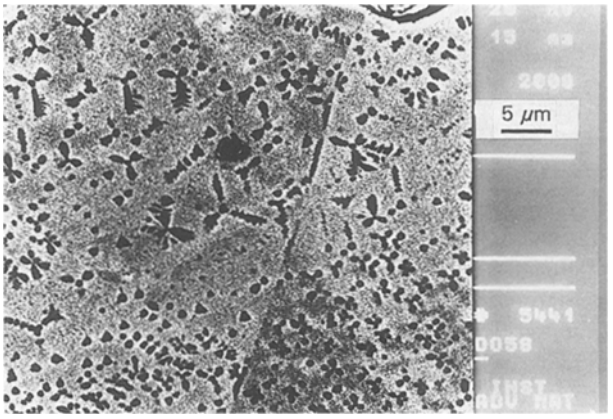

Figure 9 Trigonal intermetallic particle morphology.

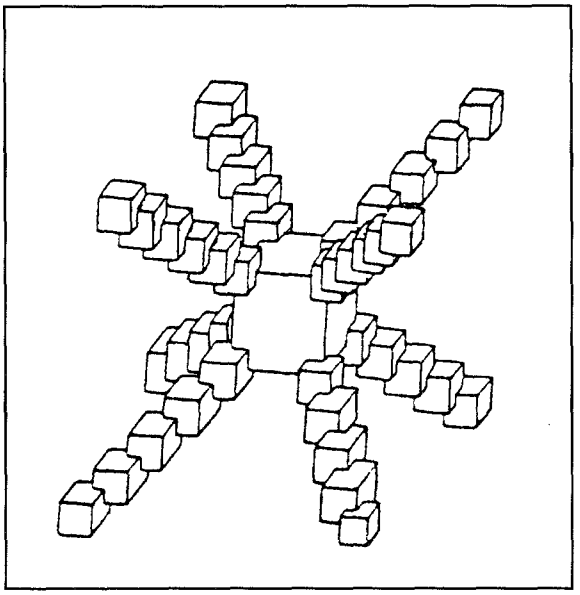

Figure 10 Schematic illustration of the cube corner growth, mechanism proposed for γ' particles.

seems to be consistent with the metallographic observations as not only was the width of the particle containing zone seen to increase with time, but the quadrifid and trigonal particle morphologies observed during structural analysis were also encountered by Westbrook when γ' containing alloys were sectioned at the appropriate orientation.

The thin intermetallic band separating the particle containing zone and the large intermetallic phase is

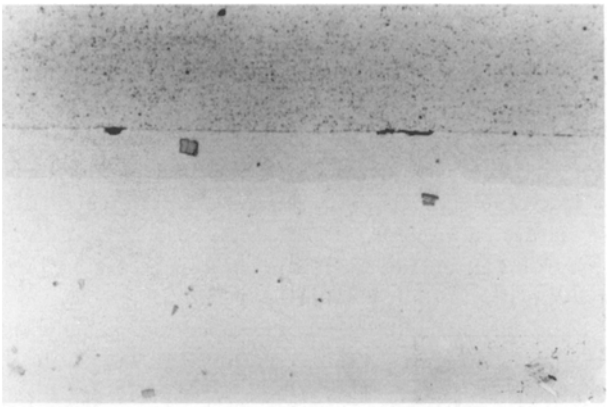

Figure 11 The microstructure present after bonding MA956 to alloy 800H (× 500).

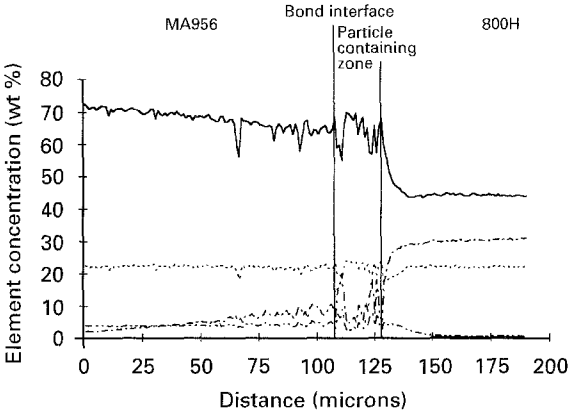

Figure 12 Elemental line plot for the MA956/800H diffusion bond; Fe (——), Cr (-------), Ni (— — —), Al (— — — —).

clearly identifiable in both Figs 6 and 7, and the elemental line scan identified downward concentration profiles for both nickel and iron across its width. The nickel concentration across this region was not large enough to form the intermetallic phase, and not low enough to be part of the particle containing zone matrix. Consequently, a distinct region was formed which separated the intermetallic phase from the particle containing zone.

The metallurgical structure developed during bonding MA956 to 800H is illustrated in Fig. 11. It is apparent that the complex microstructure formed during the bonding of MA956 to Nimonic 105 was absent within the MA956/800H alloy couple. However, a particle containing zone had developed within the 800H shaft adjacent to the bond interface. Metallographic examination of this region revealed that the particles had morphological and compositional similarities to the intermetallic particles formed during bonding MA956 to Nimonic 105. Moreover, quantitative microprobe analyses of the adjacent matrices demonstrated that the compositions were extremely similar, indicating the particle containing zone and intermetallic particles formed in a similar manner as that reported for the MA956/Nimonic 105 bond.

The absence of any intermetallic phase development can be explained by examining the microprobe line scan performed across a typical MA956/800H bond interface (Fig. 12). Although compositional differences in both iron and nickel existed between MA956 and

alloy 800H, the concentration profiles were not as steep as those encountered for the MA956/Nimonic 105 bonding couple. Moreover, the iron concentration in alloy 800H was approximately 45%, compared to 1% in Nimonic 105. As the iron requirement for the formation of the intermetallic phase was shown to be approximately 20%, the complex metallurgical microstructure cannot form in the MA956/800H bond, as the iron concentration level never falls below the base composition of alloy 800H (~ 40%).

The complex microstructures developed at the joint interfaces in successfully bonding MA956 to both Nimonic 105 and alloy 800H were also produced during the bonding tests of ODM 751.

4.3. Bond strength

An internally pressurized creep test on a MA956 tubular component at 1100 °C, using the MA956/Nimonic 105 bond to make the tube pressure retaining, established that the diffusion bond could withstand 1.2 MPa pressure for 17.5 h [6]. In this instance, the bond proved to be stronger than the MA956 tube under test and satisfied the primary objective of the experimental programme. However, in order to obtain some indication of the overall mechanical strength of the joint, a tensile creep component was prepared whose design relied solely upon the diffusion bonds to transmit an axial load to the tubular component. A tensile load equivalent to an internal pressure of 2 MPa was applied to the specimen and load line extension, and therefore failure was detected after 5.25 h. Post-test examination of the test component clearly showed that one of the Nimonic 105 end caps had been pulled out of the tube a distance of 0.5 mm. Examination of longitudinal metallographic sections prepared from the fractured end revealed that failure occurred between the particle containing zone and the intermetallic phase, and not at the joint interface. This was anticipated, as micro-hardness measurements taken across the bond had previously identified this region to be the softest.

An internally pressurized creep specimen was manufactured using the MA956/800H diffusion bond to seal the tubular component, and tested to an internal pressure of 0.8 MPa at 1100 °C. Under these test conditions, the diffusion bond proved to be stronger than the MA956 tube under test, which failed after 117 h, thereby satisfying the experimental objective.

4.4. Failure analysis

The high temperature materials information obtained during the internally pressurised creep testing programme showed the hoop strength of ODM 751 to be considerably greater than MA956 [7]. This suggested that under the same bonding conditions, and similar interfacial pressures, the thinner walled MA956 tube should preferentially fail. However, this was not the case as the ODM751 tube always fractured during the diffusion bonding process and the MA956 tube did not. Such anomalous behaviour was initially attributed to the possibility that dissimilar interfacial stresses were developed in the different bond types. These stresses would be developed due to variations in the thermal expansion coefficients and the elastic moduli of MA956 and ODM751 at 1100 °C. In order to establish if any discrepancy in material constants existed at the bonding temperature, the thermal expansion coefficients of both alloys were measured using the diametral extensometry unit developed for the internal pressure testing programme [8]. The measured experimental values are presented in Table II and are compared against the manufacturers' reported data.

The results show that although the measured experimental constants differed from the manufacturers' data by a factor of approximately 2, the transverse thermal expansion coefficients of MA956 and ODM 751 were similar. More importantly, the thermal expansion coefficient measured for Nimonic 105 also differed from the manufacturers' reported data by a similar margin, which indicated that, although an element of inaccuracy may have been inherent in the measurement procedure, the relative differences between the ferritic and austenitic alloys were comparable. Therefore, as the measured thermal expansion coefficients of both ODS alloys were similar, it appeared unlikely that fracture of the ODM751 tube resulted from dissimilar thermal expansion coefficients.

The elastic moduli of both tubular materials were measured upon pressurization of the respective tubular creep test components and the constants were calculated as 27 GPa and 35 GPa for ODM751 and MA956, respectively. A low elastic moduli would be expected at such elevated temperatures; however, it is anticipated that such a small difference in the respective constants would not be sufficient enough to cause fracture of the much stronger ODM751 tube. As both the thermal expansion coefficients and elastic moduli for both alloys were assessed to be similar at 1100 °C, the interfacial pressures developed at the joint interface during the bonding process were deemed to be of a similar magnitude.

In the preparation of the highly polished mating surfaces, great care was taken to eliminate any ovality from the inside surface of the MA956 and ODM751 tubes. However, this proved to be difficult and in the majority of bonding trials a small amount of ovality always persisted. As ovality introduces localized bending stresses within the tube wall, the ability of a material to redistribute such stress concentrations, which is strain dependent, becomes important. The internally pressurized creep tests performed on both types of ODS alloy [7], highlighted the difference that existed between the rupture ductilities of the two materials. Generally, MA956 displayed rupture ductilities of 1.5–2.5%, while in one instance, ODM751 displayed a rupture ductility as small as 0.15%. Thus, the ability of ODM751 to redistribute stress enhancements produced from any dimensional variance would be limited. It therefore appears that crack development and fracture of the ODM751 tube resulted from localized ductility exhaustion at stress concentration points produced from dimensional ovality within the

tube bore. Although a small amount of ovality probably existed in the MA956 test pieces, this material was more creep ductile than ODM751 and therefore more capable of redistributing the localized stresses produced from any dimensional irregularities. As a result, the MA956 tube did not fracture during the bonding process.

5. Conclusions

1. A solid state diffusion bonding technique was successfully employed to join tubular MA956 to both Nimonic 105 and alloy 800H using parameters derived from a series of bonding trials.
2. The successful joint design was incorporated into a tubular test piece configuration which allowed a series of internally pressurized creep tests to be performed on MA956 at 1100 °C.
3. The tube sealing joints of both the MA956/Nimonic 105 and MA956/800H diffusion bonds gave longer creep lives than the MA956 tube under internally pressurized conditions.
4. Fracture of the ODM751 tube during the bonding procedure resulted from the inability of the alloy to redistribute localized stress enhancements due to the extremely low creep ductility of the material.

References

1. B. JAHNKE and G. DANNHAUSER, in Proceedings of Conference on "High Temperature Materials for Power Engineering", edited by E. Bachelet, R. Brunetand, D. Coutsouradis, P. Esslinger, J. Ewald, I. Kvernes, Y. Lindblom, D. B. Meadowcroft, V. Regis, R. B. Scarlin, K. Schneider and R. Singer (Kluwer Academic Publishers 1990) p. 131.
2. H. D. HEDRICH, in Proceedings of Conference on "New Materials by Mechanical Alloying Techniques", edited by E. Arzt and L. Schultz (Deutsche Gesellsch, F. Metallcunde, Oberursel, Germany, 1989) p. 363.
3. Cost 501 D42 report, Ref. No. IKE-FB-170/86, 1985.
4. J. H. WESTBROOK, *Z. Kristall.* **110** (1958) 21.
5. A. J. WERONSKI and T. HEJWOWSKI, "Thermal Fatigue of Metals" (Dekker, New York, 1991) p. 96.
6. M. REES, J. D. PARKER and R. C. HURST, in Proceedings of 5th Conference on "Creep and Fracture of Engineering Materials and Structures", edited by B. Wilshire and R. W. Evans (Institute of Materials, 1993), p. 715.
7. M. REES, Ph.D. Thesis, University of Wales Swansea (1995).
8. M. REES, J. D. PARKER and R. C. HURST, in Proceedings of Conference on "Materials for Advanced Power Engineering", Part II, edited by D. Coutsouradis, J. H. Davidson, J. Ewald, P. Greenfield, T. Khan, M. Malik, D. B. Meadowcroft, V. Regis, R. B. Scarlin, F. Schubert, D. V. Thornton (Kluwer Academic Publishers, Dordrecht, The Netherlands, 1994) p. 1573.

Received 18 December 1995
and accepted 13 February 1996